79-4042

Effect of Reynolds Number on Laminar Separation of a Supersonic Stream

Odus R. Burggraf,* D. Rizzetta†
The Ohio State University, Columbus, Ohio
and
M. J. Werle‡ and V. N. Vatsa§
University of Cincinnati, Cincinnati, Ohio

Accurate numerical solutions for both interacting boundary-layer and asymptotic triple-deck equations are presented for a closed separation region generated by a compression wedge on a flat plate in supersonic flow. Interacting boundary-layer solutions were obtained for a range of Reynolds numbers from $Re = 10^4$ (where experimental verification is obtained) to $Re = 10^9$ (where agreement with triple-deck solutions is reached). These results provide insight into the development of the separating flow structure as the shear-layer thickness collapses with increasing Reynolds number. It is shown that the triple-deck model identifies the dominant length scales and important correlation parameters, and that the interacting boundary-layer model correctly approaches a triple-deck solution in the limit $Re \to \infty$, while producing accurate results at finite Reynolds number.

I. Introduction

MOST studies of laminar supersonic separation to date have employed the interacting boundary-layer concept wherein Prandtl's original equations are supplemented with an inviscid interaction law that allows the boundary layer to grow under the influence of a self-inflicted pressure gradient. The intuitive nature of arguments used to support these equations has given rise to some doubts about the reliability of this model (see Refs. 1-4 for more discussion of this issue). The rational basis for the interacting boundary-layer model has been furnished by the recent development of the asymptotic triple-deck theory,[5-11] which has been employed by Jenson et al.[12,27] to study laminar two-dimensional flow separation on a compression ramp in a supersonic stream. Comparison of these theoretical results with experiment indicates that the first-order theory overpredicts the interaction upstream of separation, although the postseparation flow properties appear to be in better agreement.[13] Thus, for practical purposes, the question arises as to the range of Reynolds numbers for which the asymptotic theory may be safely applied. A parallel study by Werle and Vasta[14] for the same problem indicates that the interacting boundary-layer model produces results in satisfactory agreement with experiment in the Reynolds number range 10^4-10^5. Noting that the interacting boundary-layer model is a one-layer composite of the triple-deck structure, it follows that its predictions should be valid at higher Reynolds numbers as well.

We analyze here in detail a particular case for an extensive range of Reynolds numbers, comparing the viscous interaction solutions obtained by Werle and Vatsa[14] with those of the asymptotic triple-deck theory as implemented by Rizzetta et al.[27] The configuration chosen for study is a flat-plate forebody followed by a wedge-compression ramp, with a slightly rounded corner taken for convenience. Numerical solutions were obtained for both theoretical models using finite-difference approximations to the governing differential equations of motion. Truncation errors were reduced by extrapolation to zero mesh size. In addition to the asymptotic comparison, results of the interacting boundary-layer theory are compared with Carter's Navier-Stokes solutions[15] and with the experimental data of Lewis et al.[16] Thus the development of the flow structure with increasing Reynolds number is clarified and the range of applicability, for practical purposes, of the triple-deck theory is established. In particular, it is found that the interacting boundary-layer model is satisfactory for any Reynolds number down to 10^4 or perhaps even lower. Most significantly, it is found that the triple-deck analysis gives a clear insight into the dependence of the interaction solutions on the physical parameters controlling the problem. It is believed that the accurate determination of surface properties (skin friction and heating levels) can be achieved only if the scaling laws identified in the asymptotic studies are closely honored in the numerical solution of either the interacting boundary-layer equations or even the Navier-Stokes equations.

II. The Triple Deck

When a boundary layer on a plane surface encounters a downstream compressive disturbance of sufficient magnitude, the flow is forced to separate from the wall. Observations show that the separation point may lie at a rather large distance ahead of the disturbance, contradicting the principle of no upstream influence inherent in Prandtl's boundary-layer theory. Using the momentum-integral method, Crocco and Lees[17] have shown that coupling the pressure disturbance of the external inviscid flow to the displacement thickness of the boundary layer permits upstream influence to be consistent with the boundary-layer equations. The formal mathematical treatment of this concept was initiated by Lighthill[18] and later developed in detail by Neiland,[5] Messiter,[7] and Stewartson and Williams.[6] All of these studies indicate that for Reynolds number $Re \to \infty$, solutions of the Navier-Stokes equations develop a multilayered structure that Stewartson has named the "triple deck." A survey of a

Received Oct. 20, 1977; revision received Oct. 16, 1978.

Index category: Jets, Wakes, and Viscid-Inviscid Flow Interactions.

*Professor, Dept. of Aeronautical and Astronautical Engineering.

†Graduate Research Assistant; presently Visiting Scientist, Air Force Flight Dynamics Laboratory (FBR), Wright-Patterson AFB, Ohio.

‡Professor, Dept. of Aerospace Engineering; presently Chief, Gas Dynamics Section, United Technologies Research Center, East Hartford, Conn.

§Postdoctoral Research Assistant; presently Research Engineer, Gas Dynamics Section, United Technologies Research Center, East Hartford, Conn.

variety of applications of this asymptotic theory is given in Ref. 19.

Figure 1 is a schematic of the triple-deck region that represents the infinite Reynolds number structure of the flow disturbance produced by a compression ramp. The scaling of the coordinates and flow variables is uniquely determined by the matching principle of the theory of matched asymptotic expansions. The longitudinal length scale of the disturbed region is of order $Re^{-3/8}$. In the transverse direction there are three distinct scalings, in each of which different physical processes dominate. The main deck (or middle layer) is simply a streamwise continuation of the upstream boundary layer; hence the thickness is of order $Re^{-1/2}$. All flow quantities here are given as small perturbations from the conventional noninteracting boundary layer. To first order, viscous forces are insignificant, and the solution of the main-deck equations can be expressed physically as a simple transverse shift of the undisturbed boundary-layer flow. Hence, flow angle and pressure are independent of transverse position in the main deck.

Since the main deck is essentially inviscid, perturbations produce slip at the wall. Hence, a viscous sublayer is established to enforce the no-slip condition. The transverse length scale in this lower deck is of order $Re^{-5/8}$. The equations of motion here reduce to the traditional boundary-layer equations. Since the layer is so thin, the density is constant to leading order and equal to its value at the wall. The slow flow in the thin lower deck responds violently to small compressive disturbances, producing relatively large vertical motion which displaces the main deck outward. The external flow is displaced in turn, and in this upper deck the flow responds as in conventional supersonic potential theory. The pressure disturbance feeding back to the lower deck is the essential link coupling the various layers together.

Thus, the solution of a compressible-flow triple-deck problem reduces to solving the traditional incompressible boundary-layer equations of the lower deck subject to a new edge condition representing the interaction with the upper deck. The mathematical problem is defined completely in Refs. 27 and 19. For the sake of the following discussion, we define here the nondimensional variables appropriate to the lower deck. Let x^*, y^*, u^*, v^*, p^*, and α^* be the physical coordinates, velocity, pressure, and ramp angle, and let X, Y, U, V, P, and α be the corresponding nondimensional quantities in the lower deck. Following Stewartson and Williams,[6] these are related as

$$x^* = x_0^* + \epsilon^3 aX, \quad y^* = \epsilon^5 bY$$

$$p^* = p_\infty^* + \epsilon^2 cP(X), \quad \alpha^* = \epsilon^2 (b/a)\alpha$$

$$u^* = \epsilon (d/b)\, U(X,Y), \quad v^* = \epsilon^3 (d/a)\, V(X,Y) \tag{1}$$

Here $\epsilon = Re^{-1/8}$ where Re is the Reynolds number, $\rho_\infty^* u_\infty^* x_0^*/\mu_\infty^*$, and x_0^* is a reference length measured to some point in the interaction region, taken here as the corner for convenience. The parameters are defined as:

$$a = x_0^* C^{-3/8} \lambda^{-5/4} (M_\infty^2 - 1)^{-3/8} (T_w/T_\infty)^{3/2}$$

$$b = x_0^* C^{5/8} \lambda^{-3/4} (M_\infty^2 - 1)^{-1/8} (T_w/T_\infty)^{3/2}$$

$$c = \rho_\infty^* u_\infty^* C^{1/4} \lambda^{1/2} (M_\infty^2 - 1)^{-1/4}$$

$$d = x_0^* u_\infty^* C^{3/4} \lambda^{-1/2} (M_\infty^2 - 1)^{-1/4} (T_w/T_\infty)^2$$

The parameter λ takes the familiar value of 0.332 when the undisturbed boundary layer is of compressible Blasius type. C is the Chapman-Rubesin constant $\rho_W \mu_W/\rho_\infty \mu_\infty$, and the other variables have their usual meaning.

To facilitate treatment of the numerical problem, the geometry was simplified by use of Prandtl's transposition theorem. New variables are introduced as:

$$Z = \begin{cases} Y \text{ for } X<0 \\ Y-\alpha X \text{ for } X>0 \end{cases}, \quad W = \begin{cases} V \text{ for } X<0 \\ V-\alpha U \text{ for } X>0 \end{cases} \tag{2}$$

The continuity and momentum equations are invariant under this change of variables. It is convenient to use the device of calculating an unsteady flow to achieve the desired steady-state solution. The pressure is eliminated from the momentum equation by differentiating with respect to Z, leading to the shear transport equation, here generalized to time-dependent flow:

$$\tau_t + U\tau_x + W\tau_z = \tau_{zz} \tag{3}$$

Here τ is the nondimensional shear stress:

$$\tau = U_Y = U_Z \tag{4}$$

which must satisfy boundary conditions obtained by matching to the main deck for $Z \to \infty$ and to the undisturbed boundary layer for $X \to -\infty$. Thus,

$$\tau \to 1 \text{ for } Z \to \infty, \quad \tau \to 1 \text{ for } X \to -\infty \tag{5}$$

U and W are obtained by integrating Eq. (4) and the continuity equation, respectively.

The surface condition on τ consistent with triple-deck theory is obtained from the viscous-interaction condition. In transposed variables, the surface ordinate can be included in Stewartson's displacement function $A(X)$, which is then defined as:

$$A(X) = \lim_{z \to \infty} (U - Z) - Y_s(X) \tag{6}$$

where $Y_s(X)$ is the surface ordinate in the original Y variable. Utilizing the pressure-displacement relation from linearized supersonic potential flow theory, the pressure gradient $P'(X)$ can be replaced by $-A''(X)$. Then, noting that U is the Z integral of τ, it is easily shown that Eq. (6) together with the boundary-layer momentum equation can be expressed in the form:

$$[\tau_z]_{z=0} = -\int_0^\infty \tau_{xx}(X,Z)\,dZ - Y_s''(X) \tag{7}$$

The set of boundary conditions on τ given by Eqs. (5) and (7) is incomplete. Despite the fact that the differential equation (3) is of paraboic type, the overall problem has an elliptic nature, indicated by the appearance of the second derivative in Eq. (7). A discussion of this point is given in Ref. 27; we merely point out here that a downstream boundary condition is required to select a unique solution from the family of branching solutions. Hence we require the disturbed

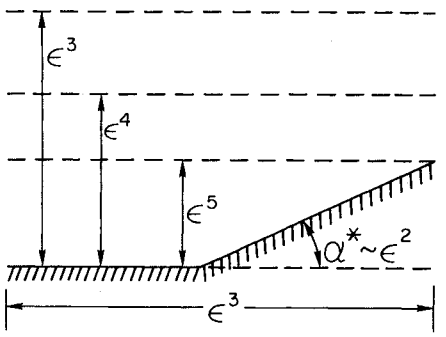

Fig. 1 Triple-deck scaling laws.

solution to decay far downstream:

$$\tau \to 1 \text{ for } X \to \infty \tag{8}$$

An equivalent condition following from Eq. (6) is that $A'(X) \to -\alpha$ as $X \to \infty$. This latter condition was not enforced, but instead was used as a test on the overall accuracy of the solution.

III. Interacting Boundary-Layer Model

In this approach, the governing equations are taken to be the classical boundary-layer equations modified only to account for a self-induced pressure gradient effect. The equations have long been used for the study of inviscid/viscous interacting flows (see Brown and Stewartson[20] for further discussion of this point), and have been found to enjoy a very wide range of applicability. These equations contain all of the displacement effects identified in second-order boundary-layer theory (see Van Dyke[21]); they apply in the classical leading-edge, strong-interaction regime (see Stewartson[22]), and it is now clear from the work of Stewartson et al.[6-11] and Burggraf et al.[12] they they contain the principal terms of the Navier-Stokes equations needed to describe small laminar separation regions. Upon review of Sec. II, it becomes clear that an interacting boundary-layer model produces a set of composite equations valid in both the main and lower decks. Unfortunately, use of this composite set of equations forces one to give up the simplicity of the universal problem identified in Eq. (2) and (7). Apparently this loss is offset by a wider range of applicability (in Reynolds number) for the composite set of equations. However, recent developments by Brown et al.[11] and Werle[23] give encouraging indications that the utility of the asymptotic models can be extended with rather straightforward modifications, a point that should be of considerable interest for future studies.

For the present study, the governing equations are employed in the form presented by Werle and Vatsa¶ (Ref. 14) in terms of the nondimensional Levy-Lees variables,

$$\xi = \int_0^s \rho_e \mu_e u_e \mathrm{d}s, \quad \eta = u_e \sqrt{Re_r/2\xi} \int_0^n \rho \mathrm{d}n \tag{9a}$$

where the subscript e refers to the inviscid edge conditions (here taken as the inviscid flow state along the displacement body), Re_r is the reference Reynolds number $\rho_\infty^* u_\infty^* x_0^* / \mu_r^*$, where μ_r^* is the viscosity evaluated at the reference temperature, $T_r^* = u_\infty^{*2}/R^*$ with R^* the gas constant, s and n are the surface and normal coordinates, respectively, given as:

$$s = s^*/x_0^* \qquad n = n^*/x_0^* \tag{9b}$$

and the dependent variables given as:

$$\rho^* = \rho_\infty^* \rho, \quad p^* = \rho_\infty^* u_\infty^{*2} p, \quad u^* = u_\infty^* u$$
$$T^* = T_r^* T, \quad v^* = u_\infty^* v, \quad \mu^* = \mu_r^* \mu \tag{9c}$$

The dependent variables are normalized as:

$$F = u/u_e \qquad \theta = T/T_e \tag{10}$$

and a normal velocity function defined as:

$$\bar{v} = [n_s F + \rho v \sqrt{Re_r/2\xi}]\, 2\xi/\xi_s \tag{11}$$

so that with the additional assumption of a linear viscosity law, the governing equations can be written as:

$$\bar{v}_\eta + F + 2\xi F_\xi = 0 \tag{12}$$

$$F_{\eta\eta} - \bar{v} F_\eta + \beta(\theta - F^2) - 2\xi F F_\xi = 0 \tag{13}$$

$$(1/Pr)\theta_{\eta\eta} - \bar{v}\theta_\eta + (\gamma - 1)/\gamma (u_e^2/T_e) F_\eta^2 - 2\xi F \theta_\xi = 0 \tag{14}$$

where

$$\beta = \frac{2\xi}{u_e} \frac{\mathrm{d}u_e}{\mathrm{d}\xi} \tag{15}$$

The boundary conditions are given as:

$$F(\xi,0) = \bar{v}(\xi,0) = 0, \quad \theta(\xi,0) = T_w/T_e \tag{16}$$

and as $\eta \to \infty$

$$F(\xi,\eta) \to 1, \quad \theta(\xi,\eta) \to 1 \tag{17}$$

The interaction effects are accounted for using the isentropic flow relations to determine the edge conditions for the pressure level established by the deflection of the mainstream as it passes over the displacement body. The displacement thickness is given as:

$$\delta = \frac{\delta^*}{x_0} = \frac{\sqrt{2\xi}}{\rho_e u_e \sqrt{Re_r}} \int_0^\infty (\theta - F)\mathrm{d}\eta \tag{18}$$

and the edge pressure is then given by linear theory** to permit the closet possible comparison with triple-deck theory:

$$p_e = p_\infty + [(\mathrm{d}y/\mathrm{d}x)_s + (\mathrm{d}\delta/\mathrm{d}x)]/\sqrt{M_\infty^2 - 1} \tag{19}$$

where $(\mathrm{d}y/\mathrm{d}x)_s$ is the local surface angle and x, y are Cartesian coordinates nondimensionalized with x_0^*. Use of this last relation with Euler's equation allows one to determine the local value of the pressure-gradient parameter β of Eq. (15). It remains only to supply appropriate initial conditions (far ahead of the ramp) and downstream conditions (far down the ramp surface) to close the problem.

Far from the ramp-juncture point it is assumed the flow is in a weak-interaction state with the local mainstream. Upstream of the ramp on the flat-plate portion of the surface, this condition is approximated by first determining the noninteracting boundary-layer solution, then determining the weak-interaction pressure and pressure gradient from the square-root growth law for the displacement thickness, and finally recalculating the initial profiles using a local similarity approach. Far aft of the ramp juncture, the weak-interaction state is applied, in an approximate sense, by requiring that the local pressure gradient decay to its inviscid level. Obviously, this approximation improves as the point of application is moved aft along the downstream wedge surface.

IV. Numerical Methods

A. Triple Deck

The numerical algorithm for interior mesh points is based on the unsteady equation of motion, Eq. (3), marching forward in time from an initial state of uniform shear flow until a final steady solution is achieved. A partially time-implicit scheme is used because it was found to be more efficient than the explicit version. The scheme used is based on

¶It is not intended to imply that the method used here is the only interacting boundary-layer method available (see Ref. 36, for example).

**For the comparisons of Fig. 3, §V, Eq. (19) was replaced by a tangent wedge-pressure law with no new complication.

backward differences in time, replacing Eq. (3) by

$$\tau_t + \Delta t[\hat{U}\tau_{tX} + \hat{w}\tau_{tz} - \tau_{tzz}] = -[\hat{U}\hat{\tau}_x + \hat{w}\hat{\tau}_z - \hat{\tau}_{zz}] \tag{20}$$

The circumflex denotes variables evaluated at the preceding time step. The X derivatives in Eq. (20) are evaluated by "windward differences" corresponding to the physical propagation of disturbances in the flow direction. Z derivatives are evaluated by centered differences.†† Thus the difference scheme is first-order accurate in ΔX and second-order accurate in ΔZ. At each X station, a tridiagonal matrix equation is solved for the new values of τ_t for each time step. The upstream and downstream boundary conditions in Eqs. (5) and (9) are replaced by the known asymptotic expansions for large X to reduce the error incurred by applying these conditions at the finite edges of the mesh. This asymptotic treatment is especially important downstream owing to the slow algebraic decay in X.

The central feature of the numerical procedure is the X-implicit treatment of the compatibility condition. Equation (7) can be expressed in finite-difference form; after premultiplying by ΔX, we find:

$$\Delta X[\tau_{i,2} - \tau_{i,1})/\Delta Z] = -(\Delta Z/\Delta X)[(\tau_{i-1,1} - 2\tau_{i,1} + \tau_{i+1,1})/2 + \sum_{j=2}^{N}(\tau_{i-1,j} - 2\tau_{i,j} + \tau_{i+1,j})] + \Delta Y'_{si} \tag{21}$$

Here $\tau_{i,j}$ refers to τ at the ith X station and the jth Z station, $j=1$ refers to $Z=0$. $\Delta Y'_{si}$ is the change of surface slope over one mesh interval, ΔX, centered at the grid point X_i. For a smooth surface (Y''_s continuous) the truncation error is of order $(\Delta X)^2$ everywhere.

We now regard Eq. (21) as an implicit-difference equation in X for determining the wall values of τ after the interior values are obtained from Eq. (20). Rearranging the terms, a tridiagonal matrix equation is obtained:

$$\tau_{i-1,1} + 2D\tau_{i,1} + \tau_{i+1,1} = 2E_i \tag{22}$$

where

$$D = -[1 + (\Delta X/\Delta Z)^2] \tag{23a}$$

$$E_i = -\{\tau_{1,2}(\Delta X/\Delta Y)^2 + \sum_{j=2}^{N}(\tau_{i-1,j} - 2\tau_{i,j} + \tau_{i+1,j}) + \Delta Y'_{si}(\Delta X/\Delta Z)\} \tag{23b}$$

The implicit nature of Eq. (22) provides interaction of all the shear profiles at each time step, permitting the necessary upstream influence, but suppressing downstream growing eigenfunctions that would develop if the solution were generated by the conventional method of marching in the X direction.

B. Interacting Boundary Layer

The method used for solving the interacting boundary-layer equations was similar in principle to that just presented for solution of the triple-deck equations in that it involved a timelike relaxation of the governing equations toward a steady-state solution of a boundary-value problem. Here, however, the equations was solved in primary variables and the time-derivative term introduced only in the pressure gradient term of the longitudinal momentum equation, the β term of Eq. (13) (see Ref. 14 for more detail). In the present version of the algorithm originally presented by Werle and Vatsa[14] three changes have been made for purposes of simplification and accuracy (also, see Ref. 23 for further discussion).

The first modification involves the multiplier h^* defined in Eq. (13b) and used in Eq. (10b) of Ref. 14, which has now been set to unity with no loss in generality. This serves to remove an unnecessary nonlinearity from the numerical equations and thus simplify the iteration process.

The second modification involves the method used to evaluate the pressure and pressure gradient through Eq. (19). Near the juncture of the compression ramp and the flat plate, the surface-slope term $(dy^*/dx^*)_s$ experiences large gradients (which are infinite if the corner is perfectly sharp). If the pressure and pressure gradient is to be continuous and smooth as verified by experiments), the displacement-thickness derivative must have offsetting but equally large derivatives in this region. Therefore, to avoid unnecessary and unacceptable truncation errors in a finite-difference representation of such terms, some accommodation must be made. This is handled through the use of total displacement body height as the sum of the surface ordinate y_S and the boundary-layer thickness δ:

$$y_{DB} = y_S + \delta \tag{24a}$$

Thus, Eq. (19) becomes

$$p_e = p_\infty + \frac{dy_{DB}}{dx}\Big/\sqrt{M_\infty^2 - 1} \tag{24b}$$

where a finite-difference representation of the derivative dy_{DB}/dx is found to produce much smaller truncation errors and, therefore, a considerably more accurate solution for a given mesh size than that presented in Ref. 14. (Note that this approach provides a result that is completely consistent with the requirements of matched asymptotic expansions, whereas the use of the dividing streamline to define the interaction surface (as proposed in Ref. 36) would not be.)

The third and final modification of the algorithm involves a simplification for purposes of economy. In reverse-flow regions, a simple analysis indicates that some sort of upwind-difference scheme is necessary to stabilize the computations. However, numerous previous studies have successfully applied the "artifical convection" concept introduced by Reyhner and Flugge-Lotz[3] to simplify the calculation procedure. This simplification reduces computer storage requirements, and was found through a comparative step-size study to produce essentially the same results for small separation regions as the upwind scheme used in Ref. 14, at least to within the accuracy to which they could be plotted. Thus, all results presented here were calculated using the artificial convection scheme as presented in Refs. 25 and 26.

V. Results

The geometry chosen for this study is the smoothed compression corner previously employed by Werle and Vatsa.[14,24,25] The form of the ramp equation is virtually identical in both physical and lower deck variables, and is given for $X > X_a$ as:

$$Y = \frac{\alpha(X - X_a)^3}{(X - X_a)^2 - X_a(X - X_a) + X_a^2/4} \tag{25}$$

where X_a is the location of the start of the ramp, taken here as $X_a = -0.3$. Note that in physical variables this point shrinks toward the corner as Re increases and, simultaneously, the physical ramp angle decreases as $Re^{-1/4}$ [(Eq. (1)]. The curved-ramp and straight-ramp geometries are compared in Fig. 2.

In order to firmly establish the level of confidence and ranges of applicability for the finite and infinite Reynolds

††The original scheme reported in Ref. 12 used windward differences for both X and Z derivatives in the inertia terms, resulting in truncation errors of first order in both ΔX and ΔZ. The present scheme allows improved results when extrapolating numerical solutions to zero mesh size.

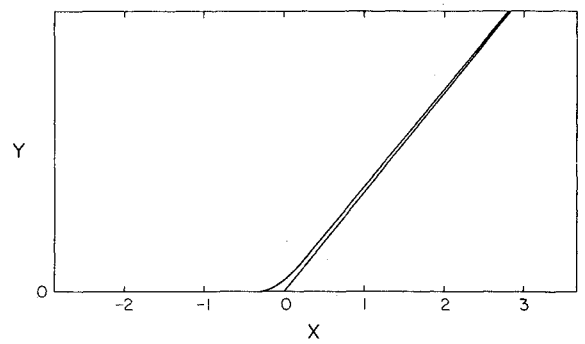

Fig. 2 Compression ramp geometry.

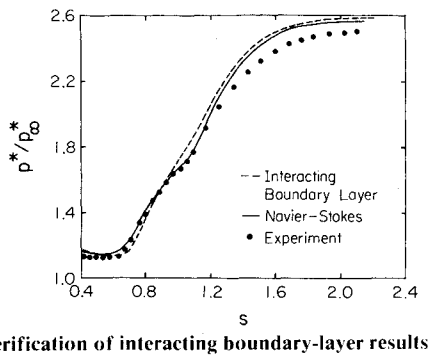

Fig. 3 Verification of interacting boundary-layer results at moderate Reynolds number.

number models, the present results will be presented in two phases. First, the interacting boundary-layer model will be assessed through a comparison with numerical Navier-Stokes solutions and experimental data at the relatively low Reynolds number of 6.8×10^4. Second, a study will be made of the influence of $Re\to\infty$ on the interacting boundary-layer model to ascertain that it properly captures the asymptotic triple-deck structure. It will become apparent that the asymptotic solutions provide critical information on the scaling of the separation problem that must be honored to obtain reliable interacting boundary-layer solutions.

For the basic assessment of the interacting boundary-layer model, comparison has been made with the Navier-Stokes solution of Carter.[15] Carter obtained accurate solutions for several sets of test conditions, one of which corresponds exactly to the experimental data of Lewis et al.[16] taken on a 10-deg compression surface at $M_\infty=4$, $Re_\infty=6.8\times10^4$, and for an adiabatic wall state. Results were obtained here for the same conditions using a generalized version of the tangent-wedge law to model the inviscid flow and Sutherland's viscosity law to determine the viscosity level throughout the flowfield (see Refs. 14 and 26 for further discussion of these points). Since Carter's solutions[15] were obtained with a finite-difference scheme that was second-order accurate in the longitudinal direction, comparison of the present first-order accurate results was made only after extrapolation in Δs to achieve the same level of truncation error.‡‡ Solutions were first obtained using step sizes of $\Delta s=0.02$, 0.015, and 0.010 and the resulting surface properties extrapolated to zero mesh width. Three values of Δs were employed to insure that Δs was sufficiently small to justify linear extrapolation. The resulting surface-pressure distributions are shown in Fig. 3 along with the Navier-Stokes solution and experimental data. The interacting boundary-layer solution compares very well with the Navier-Stokes solution of Carter, except for the lack of a slight inflection that appears at the corner in Carter's results. This difference is due most likely to the smoothed corner used in the Werle-Vatsa program. [In the limit $Re\to\infty$, computations based on the triple-deck equations indicate that the pressure distribution on the curved ramp, Eq. (25) is nearly identical to that on the straight ramp, deviating by less than 1% for $\alpha=2.5$.] The disagreement between the theoretical and experimental data downstream is not felt to be significant since the experimental pressure rise fails to reach the inviscid value for the 10 deg wedge. Note that the experimental configuration was actually a cylinder with a conical flare and, as such, exhibited an axisymmetric relief effect aft of the corner. We conclude that the interacting boundary-layer model is satisfactory for Reynolds numbers in the range 10^4-10^5.

It remains now to determine the relationship of the interacting boundary-layer model to the asymptotic triple-deck model. A test case of $\alpha=2.5$ was chosen for this comparison, corresponding to a moderately separated flow. (As shown in Refs. 27 and 28, extensive separation with a pressure plateau begins at about $\alpha=3$.) Freezing α at a fixed value permits comparison with Re as the only varying parameter. Flow conditions were taken as those of air at $M_\infty=3$, $T_{0_\infty}=868$ K, $T_w=434$ K (cooled wall), and Prandtl number of 0.71. For these conditions, the physical ramp angle varies from 14.8 deg at $Re=10^4$ to 0.83 deg at $Re=10^9$, as required by Eq. (1). The numerical results obtained for both the triple-deck and interacting boundary-layer approaches were extrapolated in longitudinal mesh size to achieve second-order accuracy. A linear variation with Δs is necessary for valid extrapolation, thus providing a severe control on step-size selection. (Sample extrapolations and tabulated results are given in Ref. 27.) At high Reynolds number extremely small step sizes were needed to achieve reliable results with the interacting boundary-layer program. In fact, accuracy could be maintained only by shrinking the computational mesh according to the triple-deck scaling laws; otherwise, numerical solutions were obtained that, while appearing acceptable, were actually too inaccurate to use.

The resulting surface pressure and skin friction distributions are shown in Figs. 4 and 5 for Reynolds numbers of 10^4 and higher. The solutions are plotted in lower deck variables to permit comparison with the unique limit solution. The triple-deck solution is approached very slowly as Re increases, especially upstream of the corner. Here the interacting boundary-layer results display a region of weak interaction that, as expected, diminishes as Re increases, disappearing altogether in the asymptotic theory. It is surprising that the region of strong interaction caused by the ramp is even shorter at finite Re than predicted by the triple-deck theory.

Some details of the flow profile properties are presented in Fig. 6 in terms of the shear distribution across the boundary layer in lower-deck variables. The limit solution in these variables shows a monotonic increase of the shear from its reverse-flow level at the wall to its outer value of one, matching to the base of the main deck. The finite Reynolds number solutions are seen to systematically approach this limit solution as Re increases. This is especially true in the lower reaches of the profiles where the region of increasing shear closely follows form of the asymptotic solution. In the outer reaches, the finite Reynolds number results are contaminated by the main deck structure with the shear dropping from peak to edge values very rapidly. This, of course, represents a finite Reynolds number effect and it can be seen that as $Re\to10^9$ the interacting boundary-layer results tend toward the vertical slope exhibited in the outer reaches of the limit solution. This also can be demonstrated by monitoring the peak levels of the shear profiles as a function of Re. These results are given in Fig. 7 where it is seen that the initial trend of a decreasing peak value reverses around $Re=5\times10^7$.

The influence of Reynolds number on the velocity profile is displayed in Fig. 8 in terms of main-deck variables. As

‡‡Note that both here and in Carter's study, a second-order accurate algorithm was employed in the direction normal to the wall; consequently, extrapolation in that direction was not necessary.

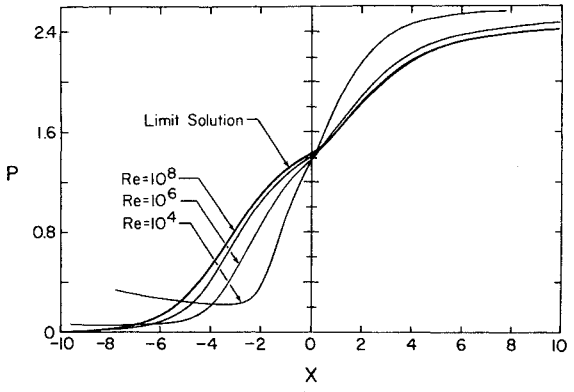

Fig. 4 Surface pressure for large Reynolds numbers for $\alpha = 2.5$.

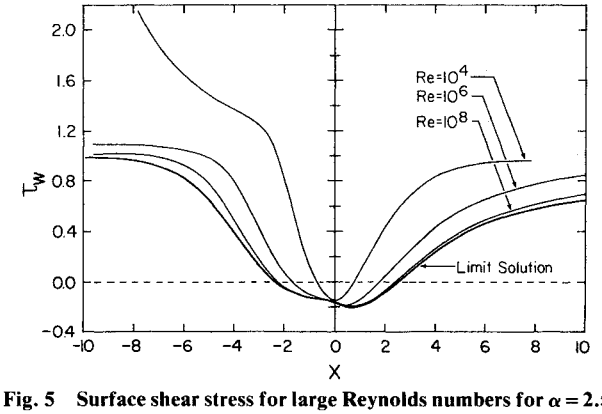

Fig. 5 Surface shear stress for large Reynolds numbers for $\alpha = 2.5$.

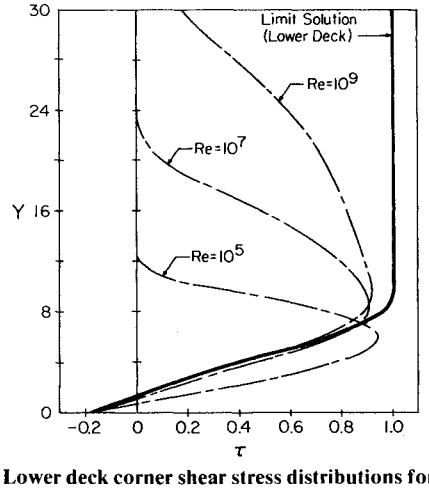

Fig. 6 Lower deck corner shear stress distributions for $\alpha = 2.5$.

discussed in Sec. II, the asymptotic solution in the main deck can be represented by an outward shifted Blasius profile. Using this concept here, the finite Reynolds number graphs have been shifted down, relative to the limit solution, by the exact amount predicted by asymptotic theory. Thus, it is made evident that as $Re \to 10^9$, the lower deck thickness decreases drastically in this scale (as it must) and the finite Re solution simply tends to reproduce the Blasius solution over the majority of the profile. It is interesting to note that the finite Re profiles parallel the asymptotic solution over a large portion of the main deck. This clearly implies that the asymptotic solution has predicted the principle variation of the flow properties and only disagrees in the amount of displacement the lower deck induces in the main-deck profiles.

Figure 9 illustrates the role of the interacting boundary-layer solution as a composite representation of the lower and

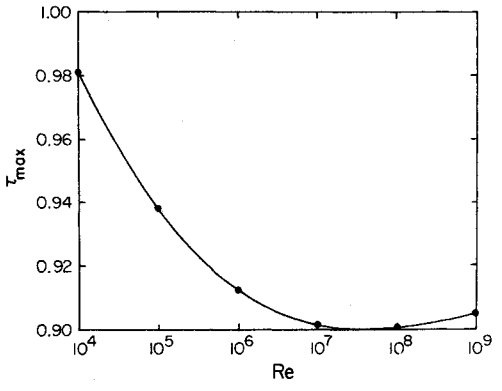

Fig. 7 Reynolds number dependence of corner station peak shear for $\alpha = 2.5$.

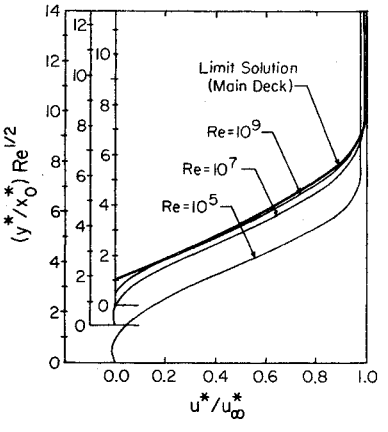

Fig. 8 Corner station longitudinal velocity distributions for $\alpha = 2.5$.

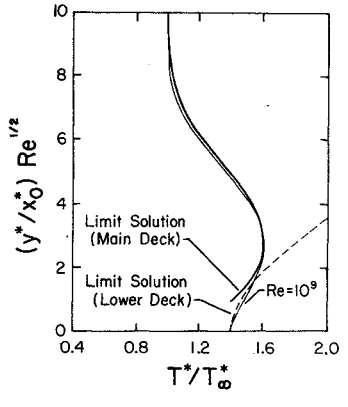

Fig. 9 Corner station static temperature distribution.

main-deck solutions of triple-deck theory. The temperature profile for the corner station is displayed here for $Re = 10^9$. The main-deck solution (Blasius solution displaced through the distance corresponding to $A(0)$ of the lower deck) agrees very well with the $Re = 10^9$ solution, as would be expected. Transfer to the lower deck profile occurs in a distance of about 10% of the overall layer thickness. Thus, accurate prediction of gradients near the wall (and thus skin friction and surface heating levels) is strongly dependent on the degree to which the lower-deck scaling is honored in choosing the computational mesh.

VI. Discussion

Our comparisons of triple-deck results with interacting boundary-layer computations for supersonic flow indicate that the asymptotic theory gives the correct qualitative trends but is quantitatively accurate only at very high Reynolds number. On the other hand, Jobe and Burggraf[29] have obtained close agreement with experiments for some subsonic

results for the trailing edge of a plate with Reynolds number as low as 10. One difference between these two cases is that the flow upstream of the disturbance is compressive in the present supersonic ramp study, whereas it is expansive in the case of the subsonic trailing edge. However, another difference that appears to be significant is the type of interaction condition appropriate to the two situations. In the supersonic case, the interaction condition is a local one that directly couples the slope of the displacement function to the pressure at the same streamwise station. In the subsonic case, the two are related through an integral equation, effectively coupling these effects at all stations simultaneously. We have shown that the principle error in velocity profiles is in the displacement produced by the lower deck (Fig. 8). This suggests that a modification of the displacement function given by Eq. (6) could lead to better accuracy at finite Reynolds number. One such approach has been presented by Tu and Weinbaum.[30] These authors introduce a more involved pressure displacement-interaction condition, but retain the condition of zero-normal pressure gradient in the lower and main decks (as in the leading approximation of triple-deck theory). The effects of streamline divergence in the main deck and compressibility in the lower deck are included as well. These latter two effects are included in the interacting boundary-layer model as well. Though formally of higher order in the asymptotic theory, they have been shown to be of equal importance to first-order terms by Brown and Williams[10] at Reynolds numbers of practical interest. Our present preference is the interacting boundary-layer model, since it contains all these terms and has been shown to give good results at both low and high Reynolds numbers and for supersonic as well as incompressible flows.

The large Reynolds numbers used in our comparisons raise questions concerning relevance to the physical world, since at the highest Reynolds numbers indicated, the physical flow would be turbulent, whereas the computations were based on laminar flow equations. This fact does not negate the worth of these comparisons, since their purpose was to demonstrate first that the triple-deck theory correctly identifies the scaling laws for interacting flows including separation regions, and second that the interacting boundary-layer model does produce the correct asymptotic flow structure for sufficiently large Reynolds numbers, thereby substantiating that the model is reliable for large but finite Re. In applications, the laminar model would be restricted to a more limited range of Reynolds numbers, especially for the adiabatic wall condition common in wind-tunnel tests. For cooled walls, transition can be delayed to very high Reynolds numbers. Theoretically, a sufficiently cold wall can maintain laminar flow at any Reynolds number for zero pressure gradient,[31] and laminar boundary layers have been observed in both free-flight and wind-tunnel tests at Reynolds numbers greater than 10^7 (Refs. 32-34). Although the pressure gradient is destabilizing in the compressive interaction region, it appears that the laminar theory has relevance at quite large Reynolds numbers if the disturbance is not too large.

In this study we have considered the case of a moderately separated flow, and have found that the interacting boundary-layer theory is a satisfactory model for that case. The question remains as to its validity for more extensive separated flows. We mention here a theoretical study by Burggraf[13] in which the mathematical structure of strongly separated flows was inferred by analyzing triple-deck numerical solutions for large-angle compression ramps (i.e., large referred to the lower deck scale). The basic features of the flow are as follows. With increasing ramp angle, the separation region with length scale $Re^{-3/8}$ is pushed upstream and a distinct postseparation pressure plateau is formed. The plateau-length scale is $\alpha^{*3/2}$, independent of Reynolds number. Thus, for α^* of order one, the separated region is extensive, with length of the same order as the length upstream of separation. The principal pressure rise occurs in the reattachment region following the plateau. The length scale here is short, of order $Re^{-1/2}\,\alpha^{*-1/2}$. For α^* small, of order $Re^{-1/4}$, the separation, plateau, and reattachment regions all have the same length scale, $Re^{-3/8}$, and hence all lie within a single triple deck. For α^* of order one, however, the three regions are distinct, each with its own scale. The reattaching flow processes are predominantly inviscid, and for large α^*, longitudinal and transverse pressure gradients are of the same order. Similar conclusions have been reached by Messiter, Hough, and Feo[35] for the case of a backward-facing step. Hence, normal pressure gradients should be accounted for when the separated region is extensive. We tentatively conclude that the interacting boundary-layer model will be applicable until the separated region extends over a length of the order of that upstream of separation.

We conclude by emphasizing a point that seems to us to be paramount—the demonstrated success of the asymptotic theory in identifying the scaling laws for separation regions. By scaling mesh size according to these laws, numerical errors were controlled, while Reynolds number was varied over an enormous range in the present interacting boundary-layer study. We strongly recommend that these scaling laws be utilized in numerical studies employing more complicated equation sets, even the full Navier-Stokes equations, in order to maintain accuracy over wide ranges of the parameters.

Acknowledgment

This work was supported by the Air Force Flight Dynamics Laboratory (Contract F33615-73-C-4014) and the Office of Naval Research (Contract N00014-76-C-0333). The authors are grateful to R. Jensen for the development of the triple-deck numerical algorithm, including the transposition of the lower-deck variables.

References

[1] Lees, L. and Reeves, B. L., "Supersonic Separated and Reattaching Laminar Flow: I—General Theory and Application to Adiabatic Boundary Layer/Shock Wave Interactions," *AIAA Journal*, Vol. 2, Nov. 1964, pp. 1907-1920.

[2] Nielsen, J. N., Lynes, L. L., and Goodwin, F. K., "Theory of Laminar Separated Flows on Flared Surfaces Including Supersonic Flow with Heating and Cooling," *Separated Flows*, AGARD Conference Proceedings N. 4, 1966, pp. 31-68.

[3] Reyhner, T. A. and Flugge-Lotz, I., "The Interaction of a Shock Wave with a Laminar Boundary Layer," *International Journal of Nonlinear Mechanics*, Vol. 3, June 1968, pp. 173-199.

[4] Georgeff, M. P., "Momentum Integral Method for Viscous/Inviscid Interactions with Arbitrary Wall Cooling," *AIAA Journal*, Vol. 12, Oct. 1974, p. 1393.

[5] Neiland, V. Ya., "Upstream Propagation of Disturbances in Hypersonic Boundary Layer Interactions," (in Russian) Akad. Nauk SSSR, Izv. Mekh. Zhidk. Gaza., No. 4, 1970, pp. 44-49.

[6] Stewartson, K. and Williams, P. G., "Self-Induced Separation," *Proceedings of the Royal Society of London*, A312, 1969, pp. 181-206.

[7] Messiter, A. F., "Boundary-Layer Flow Near the Trailing Edge of a Flat Plate," *SIAM Journal of Applied Mathematics*, Vol. 18, Jan. 1970, pp. 241-257.

[8] Stewartson, K. and Williams, P. G., "Self-Induced Separation II," *Mathematika*, Vol. 20, June 1973, pp. 98-108.

[9] Stewartson, K., "On Laminar Boundary Layers Near Corners," *Quarterly Journal of Mechanics and Applied Mathematics*, Vol. 23, May 1970, pp. 137-152; see also "On Laminar Boundary Layers Near Corners, Corrections and Addition," *Quarterly Journal of Mechanics and Applied Mathematics*, Vol. 24, 1971, pp. 387-389.

[10] Brown, S. N. and Williams, P. G., "Self-Induced Separation III," *Journal of the Institute of Mathematical Applications*, Vol. 16, 1975, pp. 175-191.

[11] Brown, S. N., Stewartson, K., and Williams, P. G., "On Hypersonic Self-Induced Separation," *The Physics of Fluids*, Vol. 18, June 1975, pp. 633-639.

[12] Jenson, R., Burggraf, O., and Rizzetta, D., "Asymptotic Solution for Supersonic Viscous Flow Past a Compression Corner," Proceedings of the 4th International Conference on Numerical

Methods in Fluid Dynamics, *Lecture Notes in Physics*, Vol. 35, Springer-Verlag, Berlin, Heidelberg, and New York, 1975.

[13] Burggraf, O., "Asymptotic Theory of Separation and Reattachment of a Laminar Boundary Layer on a Compression Ramp," AGARD-CP-168, AGARD Symposium on Flow Separation, Gottingen, Germany, 1975.

[14] Werle, M. J. and Vatsa, V. N., "A New Method for Supersonic Boundary Layer Separation," *AIAA Journal*, Vol. 12, Nov. 1974, pp. 1491-1497.

[15] Carter, J. E., "Numerical Solutions of the Navier-Stokes Equations for the Supersonic Laminar Flow Over a Two-Dimensional Compression Corner," NASA TR R-385, July 1972.

[16] Lewis, J. E., Kubota, T., and Lees, L., "Experimental Investigation of Supersonic Laminar Two Dimensional Boundary Layer Separation in a Compression Corner With and Without Cooling," *AIAA Journal*, Vol. 6, Jan. 1968, pp. 7-14.

[17] Crocco, L. and Lees, L., "A Mixing Theory for the Interaction Between Dissipative Flows and Nearly Isentropic Streams," *Journal of Aerospace Sciences*, Vol. 19, Oct. 1952, pp. 649-676.

[18] Lighthill, M. J., "On Boundary Layers and Upstream Influence. Part II. Supersonic Flows Without Separation," *Proceedings of the Royal Society of London*, A217, 1953, p. 478.

[19] Stewartson, K., "Multistructured Boundary Layers on Flat Plates and Related Bodies," *Advances in Applied Mechanics*, Vol. 14, Academic Press, Inc., New York, 1974, pp. 145-239.

[20] Brown, S. N. and Stewartson, K., "Laminar Separation," *Annual Review of Fluid Mechanics*, Vol. 1, 1969, Annual Reviews, Inc., Palo Alto, Calif.

[21] Van Dyke, M., "Higher-Order Boundary-Layer Theory," *Annual Review of Fluid Mechanics*, Vol. 1, 1969, Annual Reviews, Inc., Palo Alto, Calif.

[22] Stewartson, K., *The Theory of Laminar Boundary Layers in Compressible Fluids*, Oxford University Press, London, 1964.

[23] Werle, M. J., "Supersonic/Hypersonic Ramp-Induced Boundary-Layer Separation," Rept. No. 77-5-33, Dept. of Aerospace Engineering, Univ. of Cincinnati, May 1977.

[24] Vatsa, V. N., "Quasi-Three-Dimensional Viscid/Inviscid Interaction Including Separation Effects," Ph.D. dissertation, Univ. of Cincinnati, 1975; see also Rept. No. AFFDL-TR-75-138, Air Force Flight Dynamics Lab., Wright-Patterson AFB, Ohio, Nov. 1975.

[25] Werle, M. J. and Vatsa, V. N., "Numerical Solution of Interacting Supersonic Boundary Layer Flows Including Separation Effects," Rept. No. ARL-73-0162, Aerospace Research Labs., Wright Patterson AFB, Ohio, Dec. 1973.

[26] Werle, M. J., Polak, A., Vatsa, V. N., and Bertke, S. D., "Finite Difference Solutions for Supersonic Separated Flows," in *Flow Separation*, AGARD CP 168, 1975.

[27] Rizzetta, D. P., Burggraf, O. R., and Jenson, R., "Triple-deck Solutions for Viscous Supersonic and Hypersonic Flow Past Corners," *Journal of Fluid Mechanics*, Vol. 89, 1978, pp. 535-552.

[28] Burggraf, O. R., "Some Recent Developments in Computation of Viscous Flows," Proceedings of the 5th International Conference on Numerical Methods in Fluid Dynamics, *Lecture Notes in Physics*, Vol. 59, Springer-Verlag, Berlin, Heidelberg, and New York, 1977.

[29] Jobe, C. E. and Burggraf, O. R., "The Numerical Solution of the Asymptotic Equations of Trailing Edge Flow," *Proceedings of the Royal Society of London*, A 340, 1974, pp. 91-111.

[30] Tu, K. M. and Weinbaum, S., "A Nonasymptotic Triple Deck Model for Supersonic Boundary Layer Interaction," *AIAA Journal*, Vol. 14, June 1976, pp. 767-775.

[31] van Driest, E. R., "Calculation of the Stability of the Laminar Boundary Layer in a Compressible Fluid on a Flat Plate with Heat Transfer," *Journal of Aerospace Sciences*, Vol. 19, Dec. 1952, pp. 801-812.

[32] van Driest, E. R. and Boison, J. C., "Experiments on Boundary-Layer Transition at Supersonic Speeds," *Journal of Aerospace Sciences*, Vol. 24, Dec. 1957, pp. 885-899.

[33] Diaconis, N. S., Jack, J. R., and Wisniewski, R. S., "Boundary-Layer Transition at Mach 3.12 as Affected by Cooling and Nose Blunting," NACA TN 3920, 1957.

[34] Burggraf, O. R., "Freeflight Research on Aerodynamic Stability and Heat Transfer," WADC-TR-59-708, Part II, Aero. Res. Lab., Wright Air Dev. Center, Dayton, Ohio, 1959.

[35] Messiter, A. F., Hough, G., and Feo, A., "Base Pressure in Laminar Supersonic Flow," *Journal of Fluid Mechanics*, Vol. 60, Sept. 1973, pp. 605-624.

[36] Holt, M. and Lu, T. A., "Supersonic Laminar Boundary Layer Separation in a Concave Corner," *Acta Astronautica*, Vol. 2, 1975, pp. 409-429.